EMI filter design: Part III: Selection of filter topology for optimal performance

Article *in* IEEE Electromagnetic Compatibility Magazine · June 2012

DOI: 10.1109/MEMC.2012.6244975

1 author:

V. Tarateeraseth
Srinakharinwirot University
57 PUBLICATIONS **391** CITATIONS

EMI Filter Design
Part III: Selection of Filter Topology for Optimal Performance

Vuttipon Tarateeraseth, Member, IEEE,
Department of Electrical Engineering,
Srinakharinwirot University, Thailand.
E-mail: vuttipon@ieee.org

Abstract – In the first two parts of the electromagnetic interference (EMI) filter design series, the conducted EMI generation mechanism and the method on the measurement of noise source impedances of a switched-mode power supply were described. In this final part, the selection of filter topology for optimal performance is explained. With good accuracy of both amplitude and phase of termination impedances, an EMI filter can be designed systematically to give optimal performance.

I. Introduction

To comply with the conducted electromagnetic interference (EMI) limits, the passive EMI filter is still widely used in a switched-mode power supply (SMPS). However, one challenging task is to design the EMI filter systematically with a minimum guess. A few papers exist on systematic design procedures of EMI filters [1], [2]. The main difference between the two papers is that in [2] the noise source and load impedances are taken into account in the EMI filter design procedure, but they are not considered in [1]. Without the noise source and load impedances in the design process, it will lead to an over-designed EMI filter performance, as the filter performance is strongly dependent on the terminating impedances [3] - [5]. In this final part of EMI filter design series, a systematic and effective design procedure for the power line EMI filters to be used in SMPS applications is described [7] - [8]. The proposed procedure is validated and demonstrated by practical design examples.

II. Equivalent Circuit of EMI Filters

The structure of a typical generic filter topology of a power supply filter which is composed of common mode choke (CM choke), differential mode choke (DM choke), X-capacitors and Y-capacitors, as shown in Fig. 1. It should be noted that the most common power supply filter topology is some version of the generic filter topology [9]. The main objective of an EMI filter is to suppress the conducted DM and CM emissions generated by the SMPS and denoted as currents I_D and I_C in Fig. 1. The noise currents measured at LISN and denoted as I'_D and I'_C should be lower than the conducted EMI limit line. Like other passive filter circuits, the passive EMI filters are made from passive components; specific types of resistor, inductor and capacitor are used. More details of those components and equivalent circuits of EMI filter are described in this section.

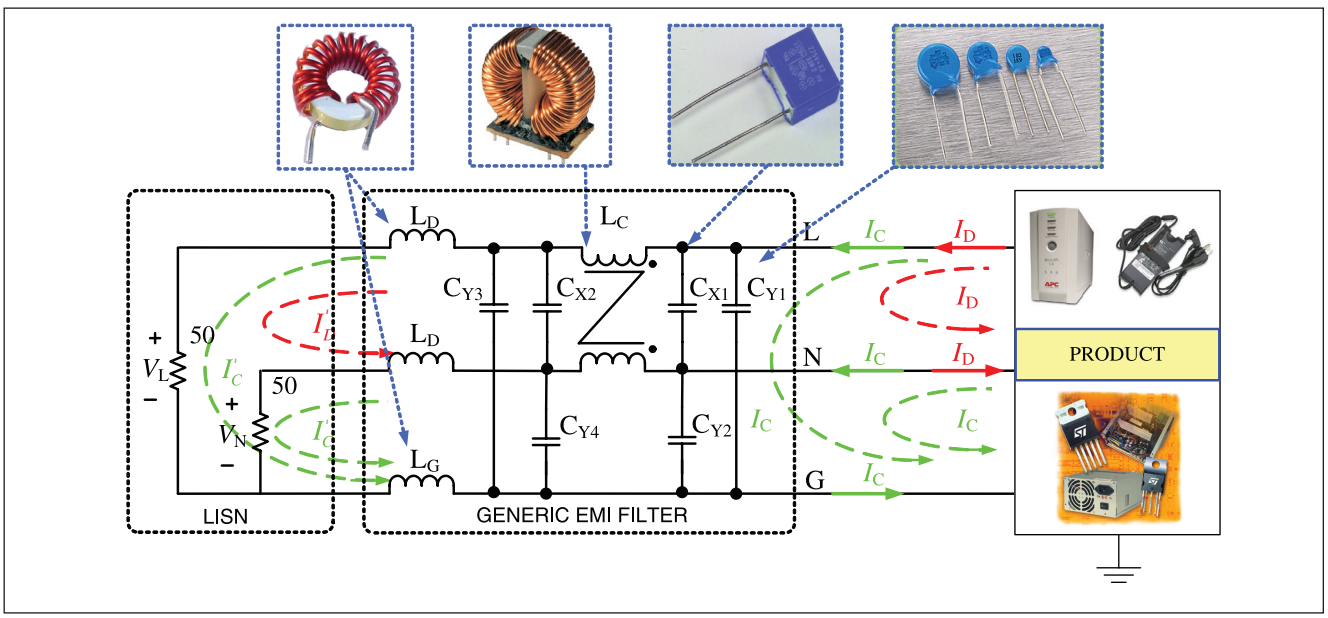

Fig. 1: The structure of a typical generic filter topology of a power supply filter.

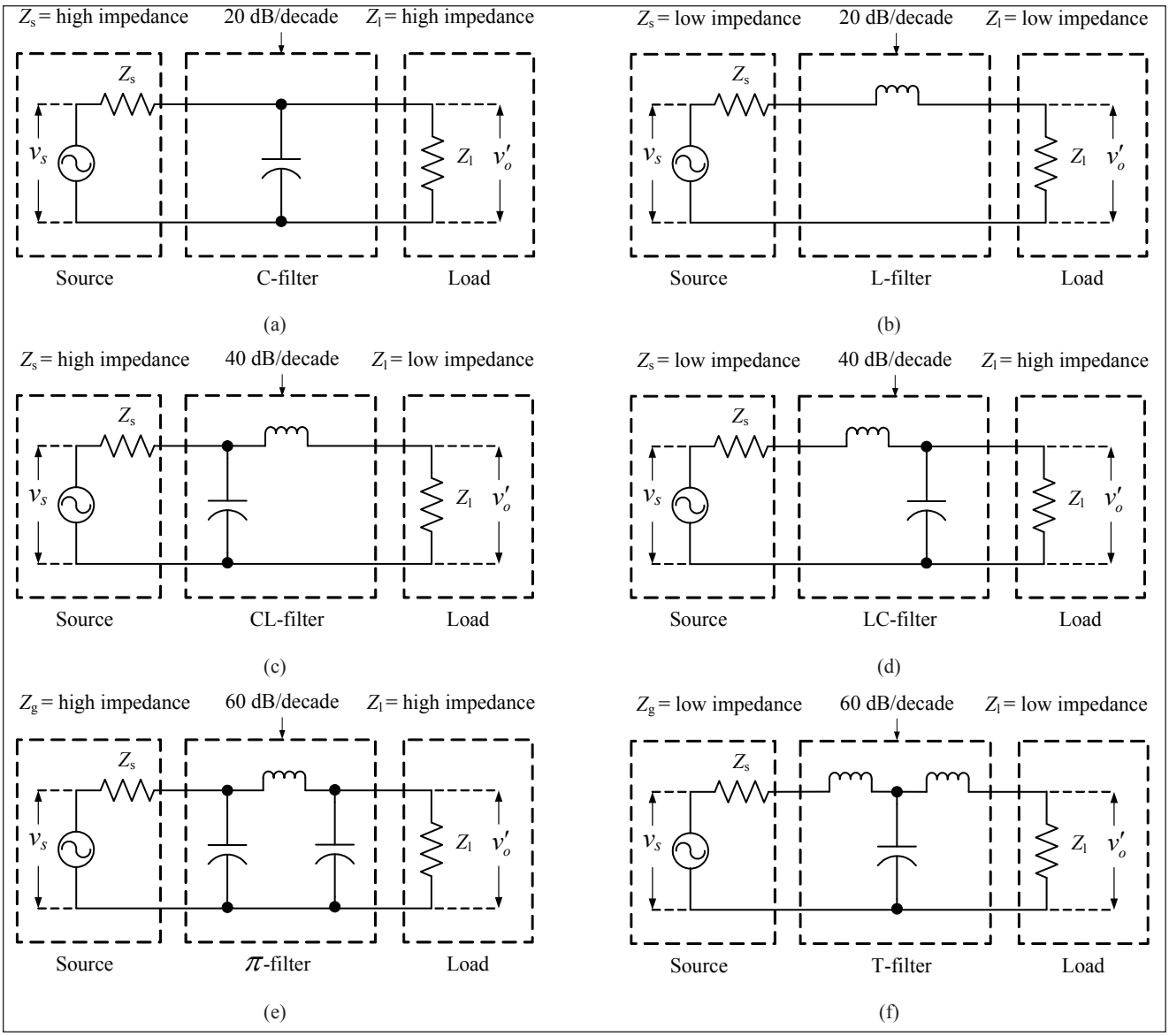

Fig. 2: Basic filter configurations. (a) C-filter; (b) L-filter; (c) CL-filter; (d) LC-filter; (e) π-filter; (f) T-filter.

Even though EMI filter circuits are diverse, they are composed of equivalent DM filters and equivalent CM filters that are based on basic filtering circuits i.e. C-filter, L-filter, LC-filter, CL-filter, π-filter and T-filter as shown in Fig. 2 [10], [11]. The basic filtering circuits provide different insertion loss (IL) rates: 20 dB/decade for C- and L-filters, 40 dB/decade for CL- and LC-filters and 60 dB/decade for π- and T-filters. However, the IL rates of the filters are strongly dependent on the impedances seen at either ends of the filters. The filter behavior can be significantly affected, if the terminating impedances at both ends are not appropriate.

The C-filter will provide 20 dB/decade IL rate with a high impedance system but it is ineffective if it is employed in a low impedance system. On the other hand, the L-filter is suitable for a low impedance system but not for a high impedance system. To gain higher IL rates, CL-, LC-, π- and T-filters need to be used. Again, to prevent the ineffectiveness of the filter performances, filter configurations should be chosen appropriately with their connecting impedances at both ends. The appropriate impedances for basic filter configurations are summarized in Fig. 2 (a) -(f).

Fig. 3 shows a typical EMI filter. It is composed of two X-caps (C_X) connecting between the line and neutral wires, two Y-caps (C_Y) connecting between both line and ground and neutral and ground wires and a CM choke (L_C). A discharging resistor is used only for discharging the (C_X) and it does not affect the noise suppression performance of the filter; thus, it can be ignored. The given EMI filter shown in Fig. 3 can be converted to the schematic shown in Fig. 4 (a). Fig. 4 (a) can be further converted to equivalent DM and CM circuits as shown in Fig. 4 (b) and (c), respectively.

Due to the DM and CM noise current directions, the CM choke and the Y-caps (C_{Y1} and C_{Y2}) affect both CM and DM emissions while the X-caps (C_{X1} and C_{X2}) affect the DM noise [12]. When the CM noise propagates through the EMI filter, the CM noise is suppressed by the

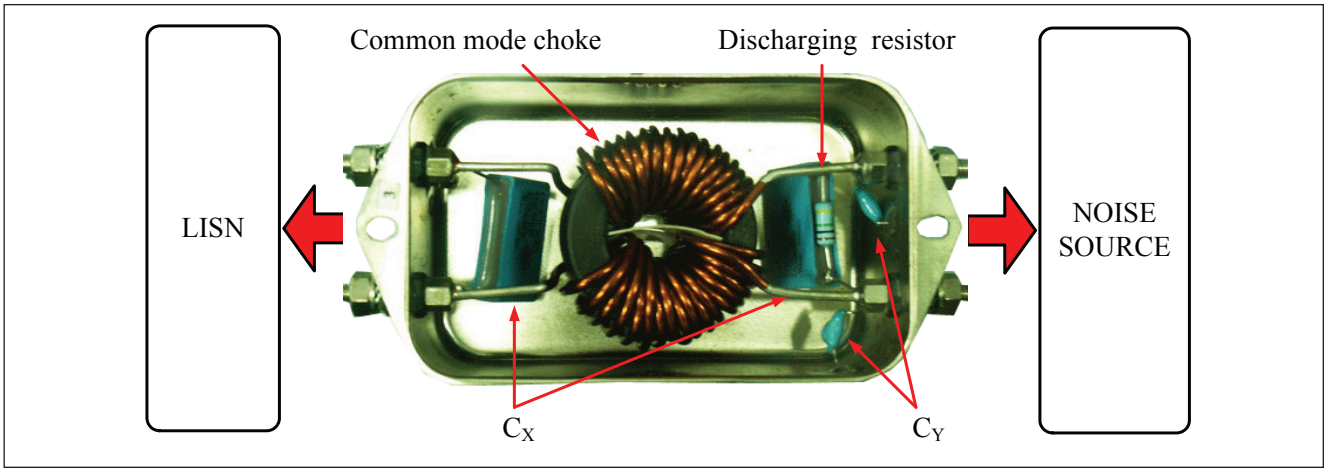

Fig. 3: Structure of a typical EMI filter.

equivalent CM filter. Since C_Y is placed by facing the noise source, the equivalent CM filter is a CL-configuration filter as shown in Fig. 4 (c). At the same time, the DM noise is eliminated by the equivalent DM filter, which is a π-configuration filter as shown in Fig. 4 (b).

The equivalent CM filter comprises of the CM inductance (L_{CM}) of the CM choke at the LISN side and the parallel of C_{Y1} and C_{Y2} (C_{YT}) at the SMPS side as shown in Fig. 4 (c). The equivalent DM filter resulted from the total leakage inductance of two windings of the CM choke ($L_{DM} = L_{lk,p} + L_{lk,s}$), the C_{X2} at the LISN and the C_{XT} at the SMPS as shown in Fig. 4 (b). As the DM noise passing through the Y-caps in series, the C_{XT} is a parallel combination of C_{X1} and the series of C_{Y1} and C_{Y2}. However, it is possible also to increase the DM noise reduction by adding the DM chokes (L_D) in series with the CM choke; in that case, the L_{DM} is a summation of the total leakage inductance and the LD.

III. Systematic EMI Filter Design

There are many factors which can deteriorate the designed EMI filter performance e.g. the termination impedances [2], [11], [12], the layout of the EMI filter components [13], and the connection between the EMI filter and a LISN [14] - [15]. In addition, the use of an EMI filter with a SMPS might perturb the overall system stability, if a DM input impedance of SMPS is larger than a DM impedance of a EMI filter connected to it [16].

Conventional filter design procedure used in communication systems and microwave applications is well developed by assuming that the terminated source and load impedances are 50 Ω matched [12], [17]. This assumption cannot directly apply to the design of SMPS EMI filters, where the actual noise source and terminated load impedances are far from 50 Ω. In practice, EMI filters are influenced by the noise source impedance and by the terminated load impedance [4] - [5], [18] and the filter design by assuming 50 Ω noise source and termination impedances leads to deviation of EMI filter performance from the actual operating conditions.

In this section, the systematic EMI filter design procedure is explained and its validation is demonstrated by the following design examples. As an example, the EMI filter is designed for the SMPS (VTM22WB, 15W, +12VDC/0.75A, -12Vdc/0.5A). The SMPS is powered through the LISN (Electro-Metrics MIL 5-25/2) following the CISPR 16-1 standard requirement. The output of the SMPS is connected to a resistive load at its full load condition. To separate the total noise into DM and CM components, the output ports of the LISN are connected to the noise discrimination network [19]. The DM and CM disturbances are monitored by the spectrum analyzer (HP 8595 E, 9 kHz - 6.5 GHz).

As shown in Fig. 5, the EMI filter design procedure can be summarized as follows. First, the DM and CM disturbances of the SMPS without EMI filter are measured; the required insertion losses ($IL_{DM,req}$ and $IL_{CM,req}$) can be determined by subtracting the emission limit from the measured DM and CM noise levels without filter. Next, the DM and CM impedances of the LISN ($Z_{LISN,DM}$ and $Z_{LISN,CM}$) and of the SMPS ($Z_{SMPS,DM}$ and $Z_{SMPS,CM}$) under its actual operating conditions must be considered. As shown in second part of EMI filter design series, the magnitude and phase of LISN and SMPS impedances were extracted and compared; as a result, the suitable equivalent DM and CM parts of the EMI filter can be chosen. Once all needed parameters are known, the equivalent DM and CM filter components can be determined using the IL formulas ($IL_{DM,estimate}$ and $IL_{CM,estimate}$). Before assembling the EMI filter prototype, the actual insertion loss ($IL_{DM,actual}$ and $IL_{CM,actual}$) are recalculated using the measured impedances of the designed EMI components.

Additionally, the power cable between the LISN and the EMI filter can also degrade the EMI filter performance at high frequency [14] - [15]. Moreover, the filter resonances and the interaction between the filter capacitor and the noise source impedance can not only degrade the EMI filter performance at high frequency but can also cause a stability problem in the SMPS. In such a case, the filters must be damped [12], [26].

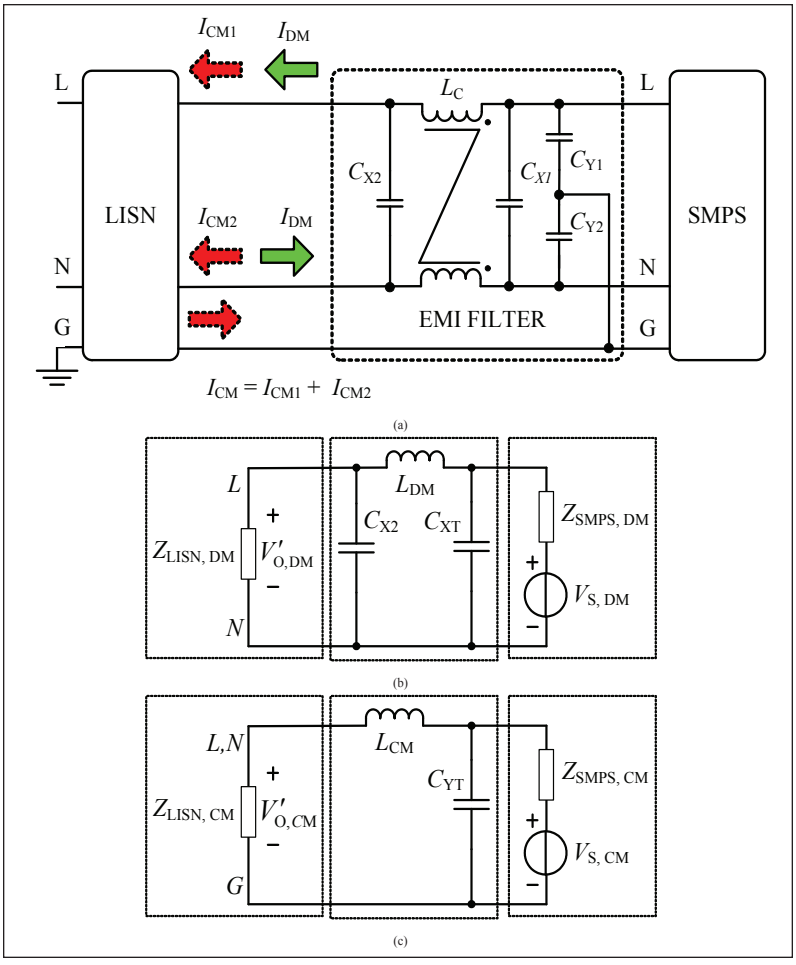

Fig. 4: Equivalent circuit of typical EMI filter: (a) schematic of Fig. 3; (b) equivalent DM filter; (c) equivalent CM filter.

Base on the knowledge of the DM and CM impedances of the LISN and SMPS as extracted previously in the second part of EMI filter design series, a step-by-step proposed procedure to design the EMI filter is given in Section IV. Finally, the effect of incorrect filter configuration to the EMI filter performance is verified in Section V.

IV. Realization # 1: Proposed EMI Filter Design Procedures For SMPS

The intended conducted EMI limit to be met by the SMPS is the CISPR 22 Class B limit [27]. The LISN specified by this standard can only measure the total conducted emissions consisting of both the DM and CM components. Therefore, a discrimination network is needed to separate the DM and CM components from the LISN so that they can be measured separately [19].

A. Determination of the required insertion losses

The conducted emissions of the SMPS without the filter are measured with the LISN alone. The measurement setup is shown in Figs. 6. The line-to-ground and neutral-to-ground conducted emissions are shown in Figs. 7 (a) and (b), respectively. Obviously, the SMPS can never meet the required EMI limit without an EMI filter. With the help of the discrimination network proposed in [19], the DM and CM conducted emissions of the SMPS without the filter are measured and shown in Figs. 7 (c) and (d), respectively. Thus, the required DM and CM filter insertion losses can be found by subtracting from the measured DM and CM emissions, given in Figs. 7 (e) and (f).

B. Selection of the DM/CM filter topologies based on termination impedances

Next step is to choose the proper EMI filter topology. From the DM and CM impedances comparison between SMPS and LISN shown in second part of EMI filter design series, it can be seen that the SMPS DM impedance magnitude is higher than that of the LISN by a few tens ohm to a few hundred ohm over the frequency range of measurements. The comparison of CM impedances shows that the CM impedance of the SMPS is much larger than that of the LISN one over the frequency range of interest. With this information, the proper EMI filter circuit can be chosen. Since the capacitor, to be effective, must be placed in parallel to a high impedance and the inductor must be connected in series with a low impedance [3], CL-filter configurations of both equivalent DM and CM filters are chosen where the X-caps and Y-caps are at the SMPS side and the CM choke is at the LISN side as illustrated in Fig. 8 (a).

The EMI filter is composed of one CM choke (L_C), one DM capacitor (C_X), and two CM capacitors (C_{Y1} and C_{Y2}). Due to the leakage inductance of L_C, the CM choke also doubles up as two DM inductors in the line and neutral lines. The DM and CM interpretation of Fig. 8 (a) leads to two separate circuits, shown in Figs. 8 (b) and (c), respectively. Fig. 8 (b) presents the DM-suppressing part of the filter and is composed by L_{DM}, which is the DM inductance due to L_C, and by C_{XT}, which represents the effective DM capacitor (C_{Y1} and C_{Y2} in series and then in parallel with C_X). Fig. 8 (c) presents the CM-suppressing part of the filter and is composed by LCM, which is the CM inductance due to L_C and by C_{YT}, which is the effective CM capacitor (C_{Y1} and C_{Y2} in parallel).

From Figs. 8 (b) and (c), the expressions of DM and CM filter insertion losses are rewritten as

$$IL_{DM,estimate} = 20\log\left|s^2\left(\frac{L_{DM}C_{XT}Z_{SMPS,DM}}{Z_{LISN,DM}+Z_{SMPS,DM}}\right)+s\left(\frac{L_{DM}+C_{XT}Z_{SMPS,DM}Z_{LISN,DM}}{Z_{LISN,DM}+Z_{SMPS,DM}}\right)+1\right|, \quad (1)$$

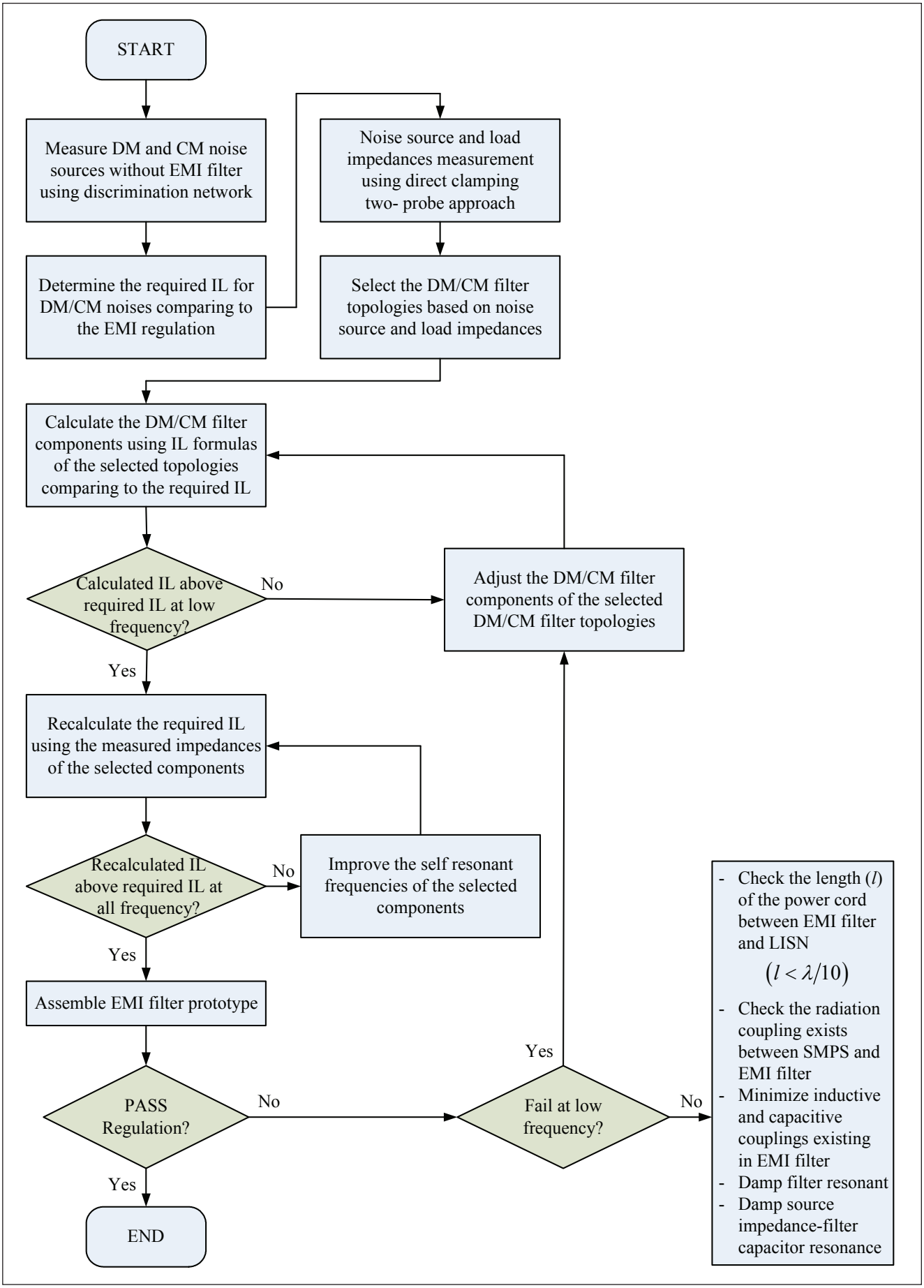

Fig. 5: Flow diagram of the proposed EMI filter design procedure.

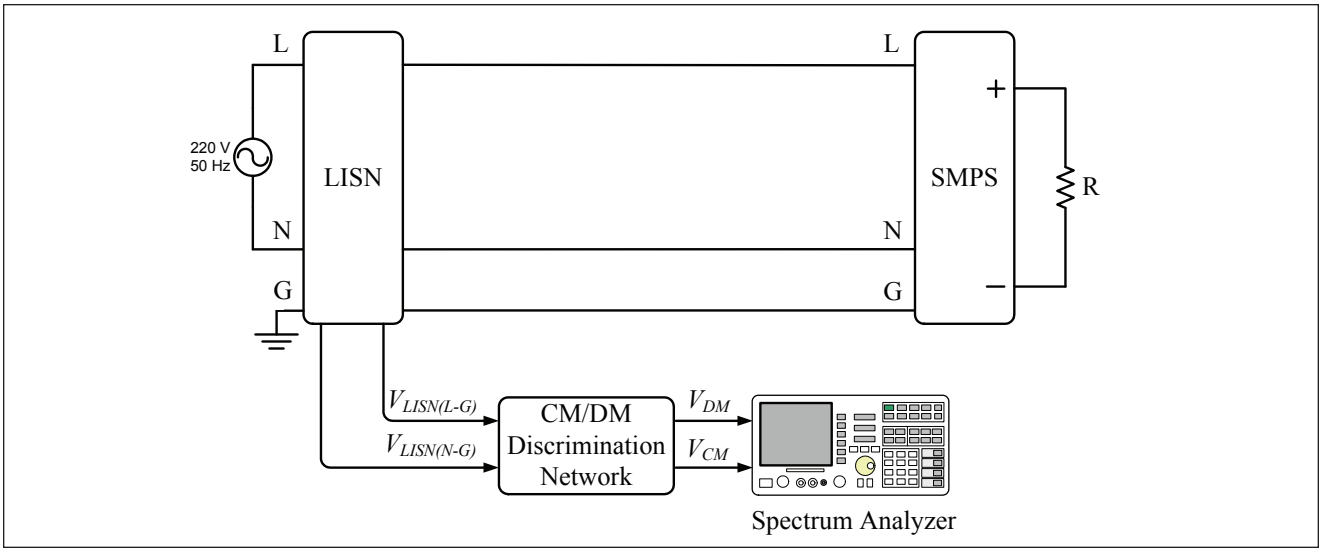

Fig. 6: Schematic of DM and CM noise measurements without EMI filter being inserted.

$$IL_{CM,estimate} = 20\log\left|s^2\left(\frac{L_{CM}C_{YT}Z_{SMPS,CM}}{Z_{LISN,CM}+Z_{SMPS,CM}}\right)+s\left(\frac{L_{CM}+C_{YT}Z_{SMPS,CM}Z_{LISN,CM}}{Z_{LISN,CM}+Z_{SMPS,CM}}\right)+1\right|, \quad (2)$$

where

$s = j2\pi f$,

f = frequency normally spanning in the conducted EMI range [Hz],

$C_{YT} = C_{Y1}//C_{Y2}$ [F],

$C_{XT} = C_X//(C_{Y1} + C_{Y2})$ [F],

L_{CM} = CM inductance of CM choke [H],

L_{DM} = Equivalent DM inductance of CM choke [H],

$Z_{SMPS,DM}$ = DM SMPS impedance [Ω],

$Z_{SMPS,CM}$ = CM SMPS impedance [Ω],

$Z_{LISN,DM}$ = DM LISN impedance [Ω],

$Z_{LISN,CM}$ = CM LISN impedance [Ω].

Based on Eqs. (1) - (2), the EMI filter component values are ready to be determined.

C. CM filter design

For the equivalent CM filter design, as shown in Fig. 8 (c), there are two unknown parameters that are the CM inductance of CM choke and the capacitance of Y-caps. Since the size of the EMI filter is strongly dependent on the size of CM choke, the Y-caps capacitance must be chosen as large as possible, to minimize the CM inductance value. The Y-capacitors are usually constrained by safety requirements, e.g. EN 60335-1 Class I portable, and therefore the maximum capacitance connected to ground cannot exceed about 4700 pF on each phase for 250 VAC 50 Hz mains [10]. Hence, C_{Y1} and C_{Y2} are chosen to be 1000 pF each. Substituting the known CM LISN and SMPS impedances and the chosen CM capacitors into (2) and assuming that the filter elements are ideal, the required CM inductance is chosen in such a way that the distance between the $IL_{CM,estimate}$ and the $IL_{CM,req}$ is minimized which is about 2 mH. Hence, two 1000 pF Class Y capacitors and a 2 mH CM choke (NEC/TOKIN SC-02-10A1) are chosen for the CM filter.

D. DM filter design

Once the CM choke and the CM capacitors are selected, the equivalent DM filter design is addressed. The equivalent DM filter, as shown in Fig. 8 (b), has two unknown parameters, i.e. DM inductance and X-caps capacitances. Because the CM choke was chosen, its DM inductance (leakage inductance) is about 17.6 μH. With this information, only the X-caps capacitance must be determined.

For X-type capacitors, since there is no safety issue, the value can be chosen as large as possible but larger capacitors usually exhibit a low self resonant frequency (SRF) and high inrush current [29]. Substituting the known DM LISN and SMPS impedances and the measured DM inductance of the CM choke into (1), the required X-cap capacitance is chosen in such a way that the distance between the $IL_{DM,estimate}$ and the $IL_{DM,req}$ is minimized: this leads to a capacitance value of about 1.5 μF.

E. Actual insertion losses and validations

Before building the EMI filter, its real performance must be assessed, and the parasitic effects of the filter components need to be considered. The impedance behavior of the filter components, chosen according to the above considerations, were measured by means of a HP 4396B impedance analyzer (100 kHz - 1.8 GHz), and the results are shown in Figs. 9 (a) - (f). The actual insertion losses of the DM and CM filters of Figs. 8 (b) and (c) can be worked out as an adaptation of (1) and (2) with the inclusion of the parasitic effects of the filter components:

$$IL_{DM,actual} = 20\log\left|\frac{Z_{C_XT}(Z_{L_DM}+Z_{LISN,DM})+Z_{SMPS,DM}(Z_{C_XT}+Z_{L_DM}+Z_{LISN,DM})}{Z_{C_XT}(Z_{LISN,DM}+Z_{SMPS,DM})}\right|, \quad (3)$$

$$IL_{CM,actual} = 20\log\left|\frac{Z_{C_YT}(Z_{L_CM}+Z_{LISN,CM})+Z_{SMPS,CM}(Z_{C_YT}+Z_{L_CM}+Z_{LISN,CM})}{Z_{C_YT}(Z_{LISN,CM}+Z_{SMPS,CM})}\right|, \quad (4)$$

where

Z_{L_DM} = Effective DM impedance of the CM choke [Ω],

Z_{L_CM} = CM impedance of the CM choke [Ω],

Z_{C_YT} = Effective CM impedance of $C_{Y1}//C_{Y2}$ [Ω],

Z_{C_XT} = Effective DM impedance of $C_X//(C_{Y1}+C_{Y2})$ [Ω].

Using the measured impedances of all the chosen filter components (shown in Fig. 9 (a) - (f)), as well as the LISN and SMPS impedance characteristics, the actual insertion losses of the DM and the CM filters (computed by means of (3) and (4)) are plotted in Figs. 11 (a) and (b), respectively. For comparison, the required DM and CM filter insertion losses are also shown in the same figures. Both the actual DM and CM filter insertion losses are higher than the required ones, which indicate that the designed EMI filter is able to suppress the DM and CM conducted emissions below the CISPR 22 Class B limit.

Finally, to verify the noise reduction performance of designed EMI filter, conducted EMI (DM, CM, L-G and N-G noise voltages) are measured when the designed EMI filter is added in. The schematic of the measurement setup are shown in Fig. 10. Figs. 11 (c) and (d) show the measured DM and CM conducted emissions after the designed EMI filter is inserted. Both the DM and CM conducted emissions are below the limit, confirming that the designed EMI filter fulfills the requirement. As a final compliance check, Figs. 11 (e) and (f) show the line-to-ground and the neutral-to-ground conducted emissions, respectively, and their results indicate that the filtered SMPS complies with the regulations limits.

V. Realization # 2: Effect of Incorrect Filter Configuration

To illustrate the effect of an incorrect filter configuration that leads to non-optimal performance of the EMI filter, the same EMI filter already designed in realization #1 is mounted in a reverse configuration; this means that the CM choke position is now shifted to the SMPS end. The new EMI filter configuration is shown in Fig. 12 (a). The equivalent DM and CM filters are LC-configuration filters as shown in Figs. 12 (b) and (c), respectively.

The actual DM and CM filter insertion losses of the LC-configuration filters can be rewritten as follows,

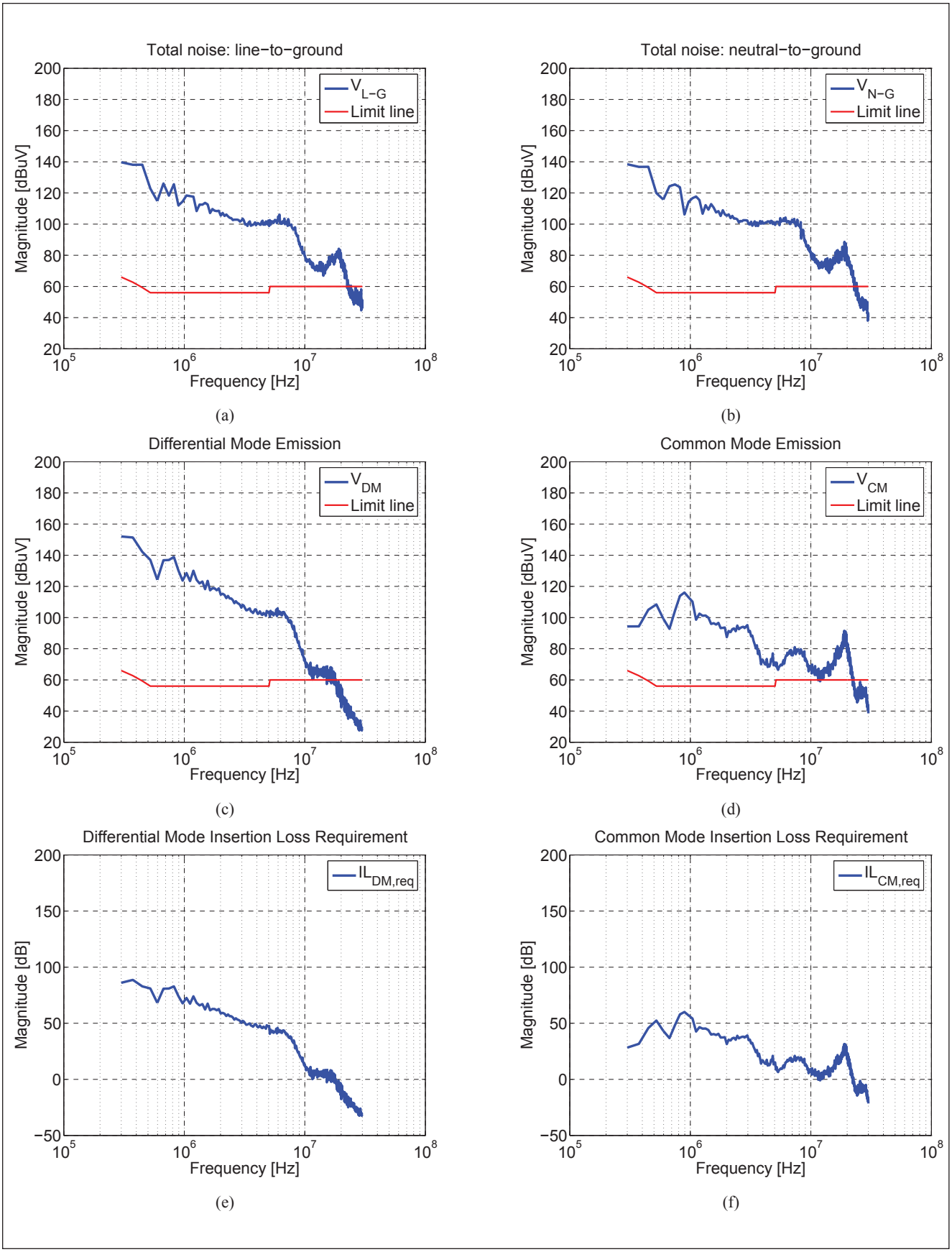

Fig. 7: Measured conducted emission without filter. (a) Line-to-ground; (b) neutral-to-ground; (c) DM; (d) CM; (e) required DM filter insertion loss; (f) required CM filter insertion loss.

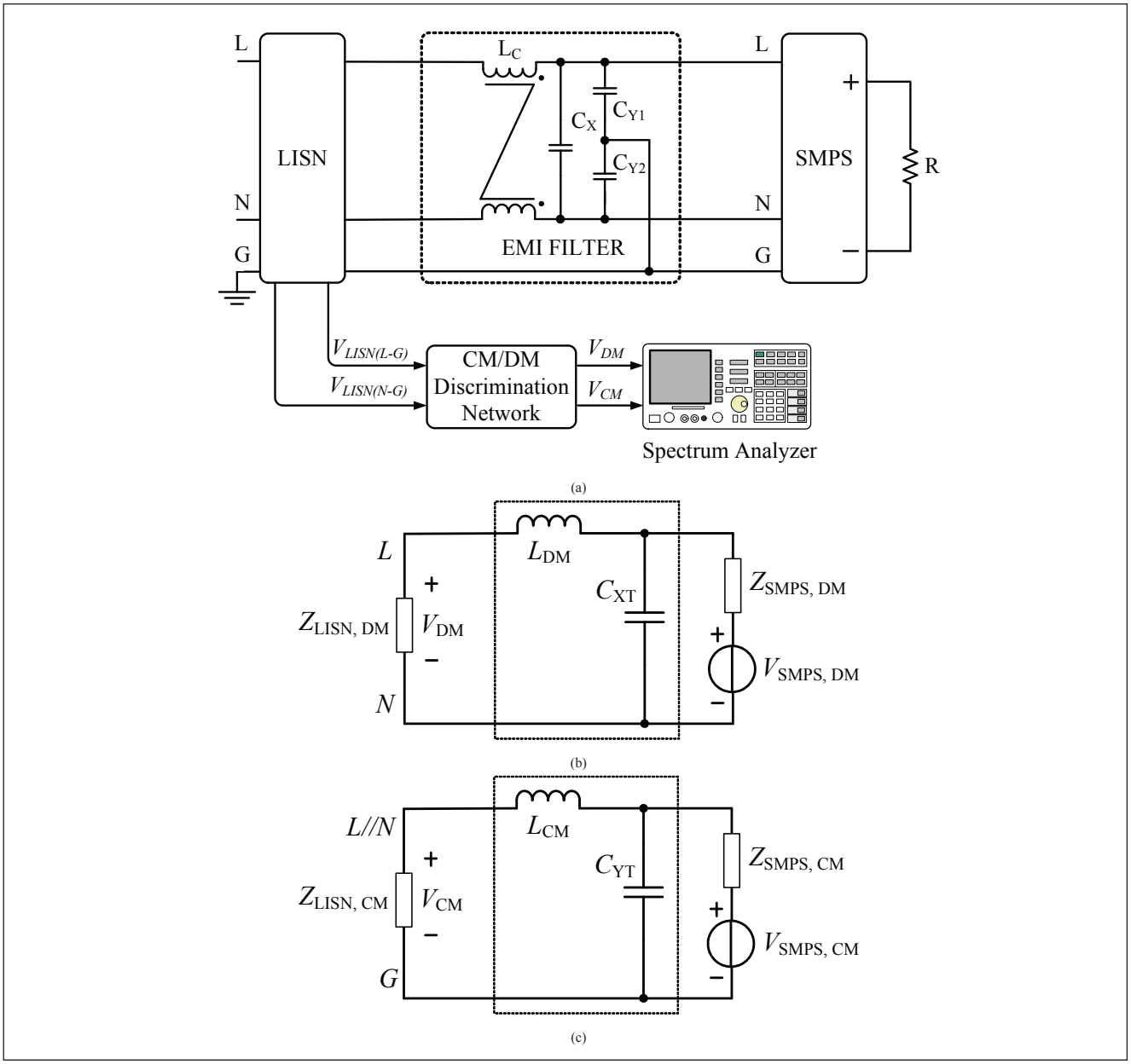

Fig. 8: Conducted EMI measurement in the presence of the EMI filter. (a) Test setup with CM/DM discrimination network; (b) DM part of the filter; (c) CM part of the filter.

$$IL_{DM,actual} = 20\log\left|\frac{(Z_{C_{XT2}}+Z_{LISN,DM})(Z_{SMPS,DM}+Z_{L_{DM}})+Z_{C_{XT2}}Z_{LISN,DM}}{Z_{C_{XT2}}(Z_{LISN,DM}+Z_{SMPS,DM})}\right|, \tag{5}$$

$$IL_{CM,actual} = 20\log\left|\frac{(Z_{C_{YT}}+Z_{LISN,CM})(Z_{SMPS,CM}+Z_{L_{CM}})+Z_{C_{YT}}Z_{LISN,CM}}{Z_{C_{YT}}(Z_{LISN,CM}+Z_{SMPS,CM})}\right|. \tag{6}$$

Based on equations (5) - (6), the actual DM and CM filter insertion losses are plotted in Figs. 13 (a) and (b), respectively. By comparing with the required DM and CM filter insertion losses, they show that the actual DM filter insertion loss deteriorates marginally at low frequency, but the actual CM filter insertion loss is unable to meet the required CM filter insertion loss below 1.8 MHz. The DM and CM conducted emissions, shown in Figs. 13 (c) and (d) respectively, confirm that the DM conducted emission exceeds the limit marginally at low frequency and the CM conducted emission exceeds the limit badly below 1.8 MHz.

Finally, the line-to-ground and neutral-to-ground conducted emissions are measured and shown in Figs. 13 (e) and (f), respectively. As the

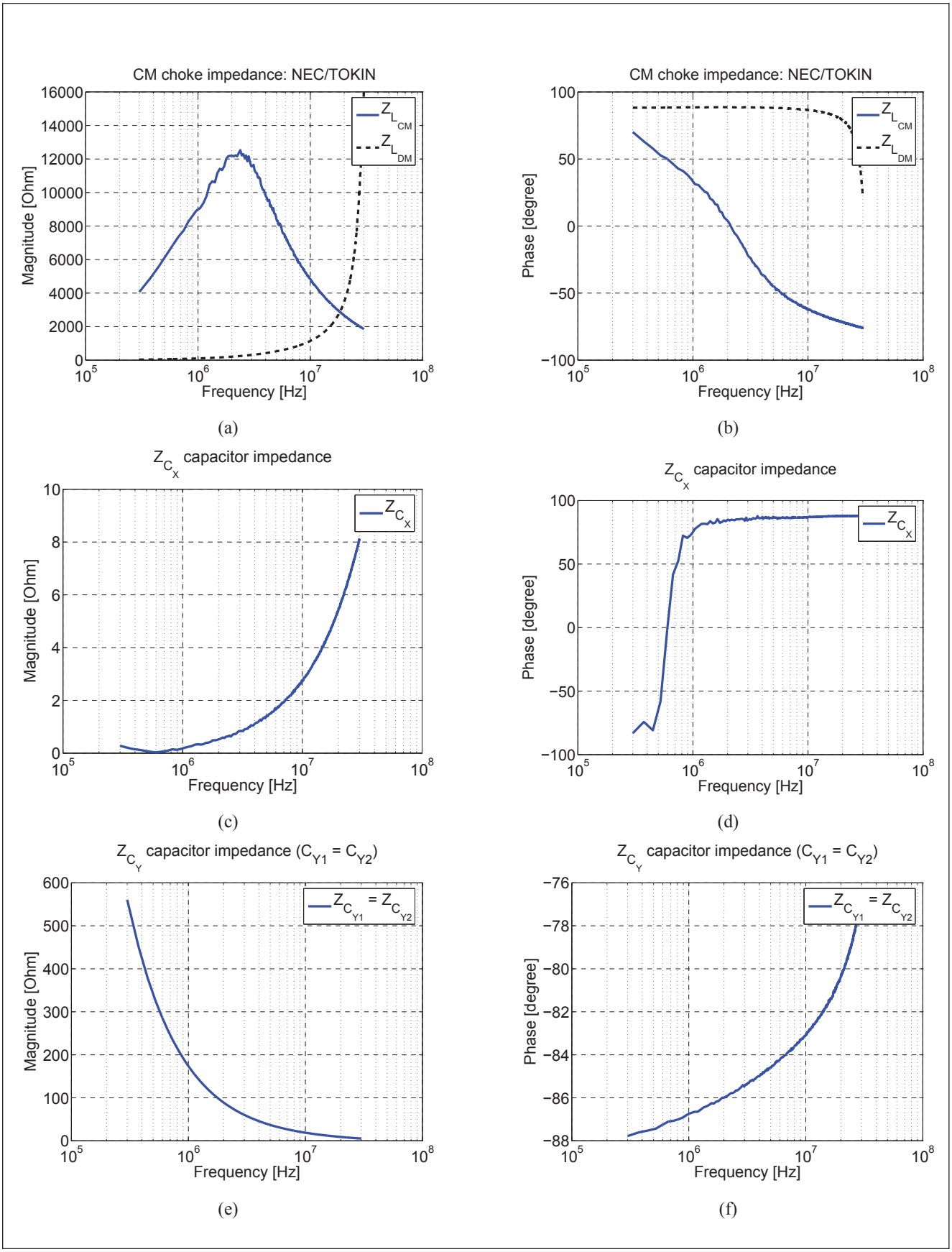

Fig. 9: Measured impedance of the chosen filter components. Plots (a) and (b) refer to the CM choke (NEC/TOKIN); (c) and (d) refer to the C_X = 1.5 µF capacitance; (e) and (f) refer to the $C_{Y1} = C_{Y2}$ = 1000 pF capacitances.

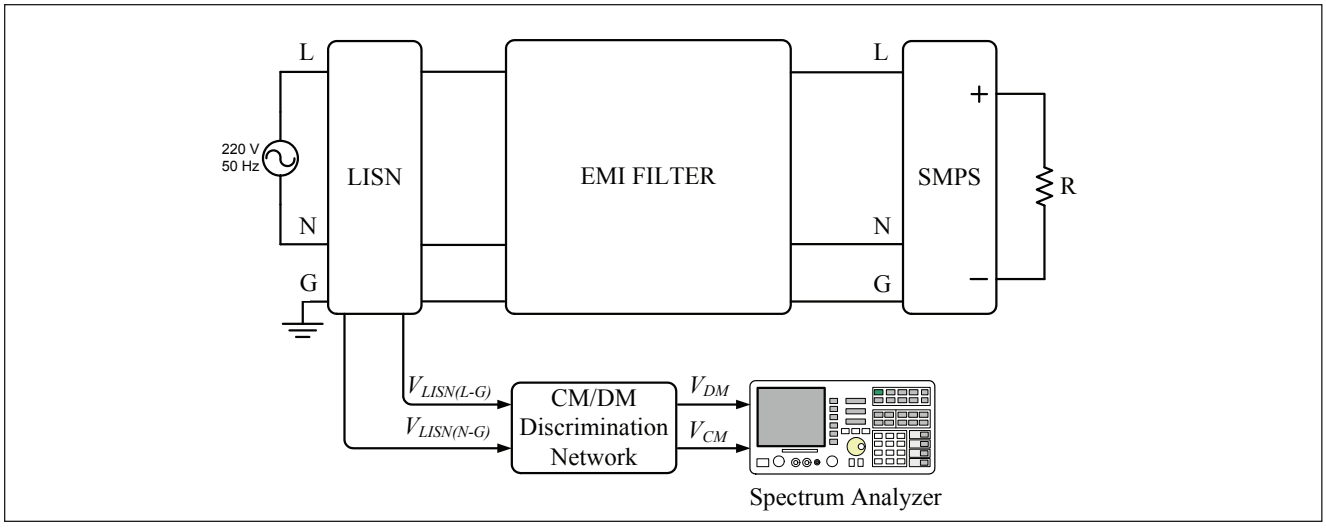

Fig. 10: Schematic of DM and CM noise measurements with EMI filter being inserted.

CM conducted emission dominates below 1.8 MHz, the SMPS does not comply with the limit at frequencies below 1.8 MHz.

VI. Conclusion

In this final article of EMI filter design series, we focus on systematic EMI filter design procedure. With known amplitude and phase information of LISN and SMPS impedances, EMI filters can be designed systematically. Using a SMPS as a practical design example, it has been demonstrated that

- The optimal filter configuration and the correct filter component values can be chosen.
- The incorrect filter configuration leads to non-optimal filter attenuation, thus causing the same SMPS to fail the required EMI limit badly.

Nevertheless, in the proposed design procedure, it is not only specific for a single-stage passive EMI filter but factors like component volume and component price are not taken into account. It might be difficult to choose between a CL-configuration of equivalent DM filter with one huge C_X (C_X = 1.5μF) and a pi-configuration with two smaller C_X ($C_{X1} = C_{X2}$ = 0.47μF) since both can comply with regulations. Optimization might be applied to take into account physical and economical parameters of the filter. The possible further applications of the EMI filter design procedure are for diverse types of systems, like three-phase AC industrial motor drives, large uninterruptible power supplies (UPS), wind turbine power stations, etc. and DC supplies, e.g. photovoltaic inverters-whose input impedances need to be determined.

For Fig. 11 – see page 71

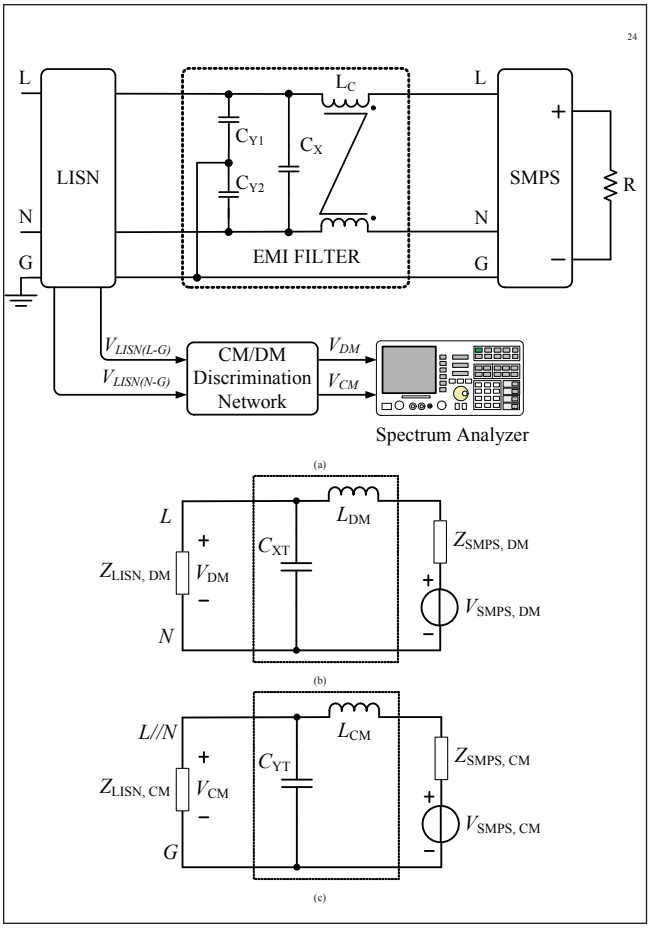

Fig. 12: (a) Realization #4: reversed EMI filter configuration. (b) DM filter; (c) CM filter.

VII. Acknowledgment

The author would like to acknowledge the useful suggestions and comments from Assoc. Prof. See Kye Yak and Prof. Flavio G. Canavero on the content of this series of articles.

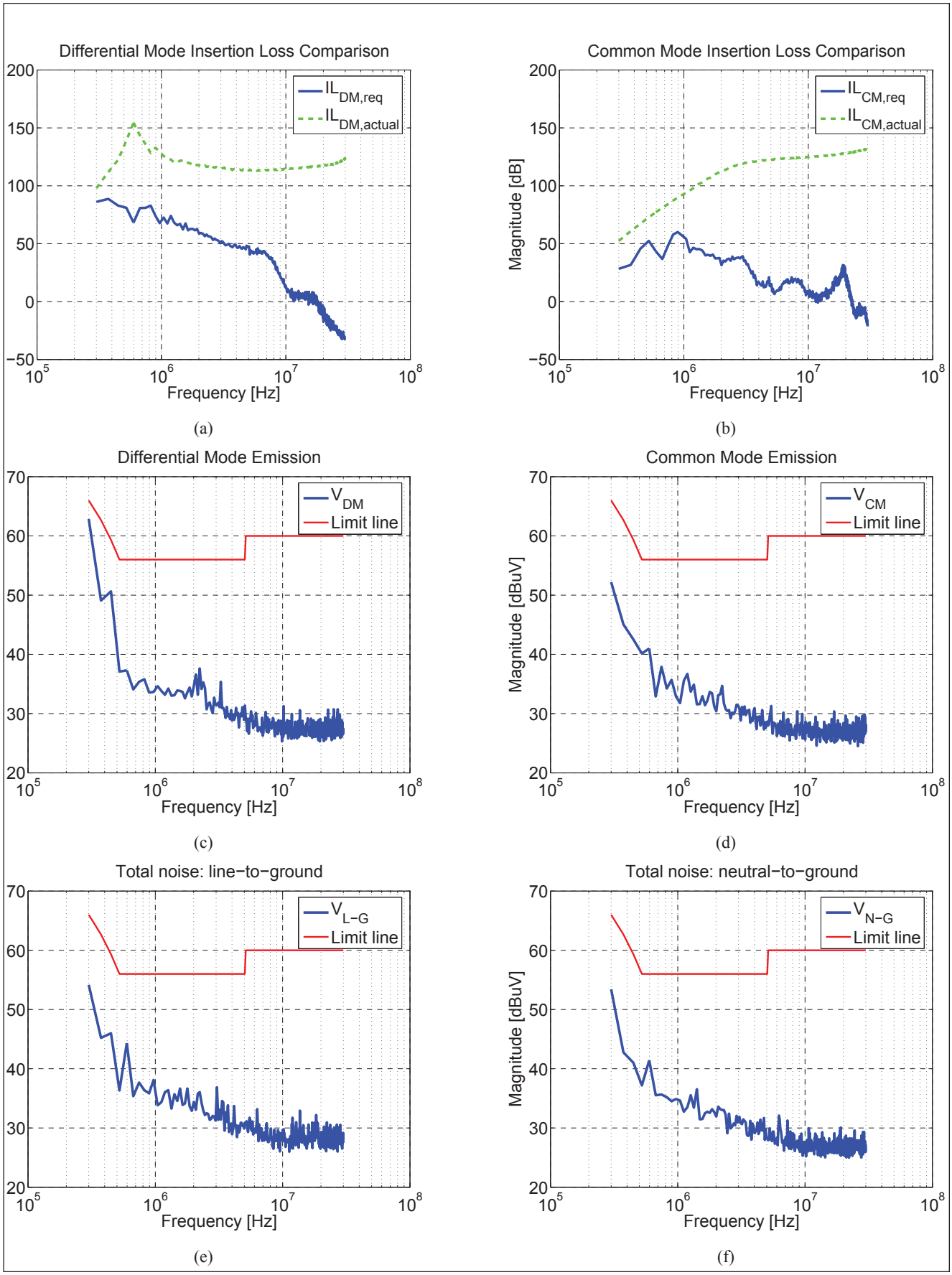

Fig. 11: Effect of the insertion of the EMI filter. (a) Required and actual DM insertion losses; (b) required and actual CM insertion losses; (c) measured DM conducted emission with filter; (d) measured CM conducted emission with filter; (e) measured total conducted emissions for line-to-ground; (f) measured total conducted emission for neutral-to-ground.

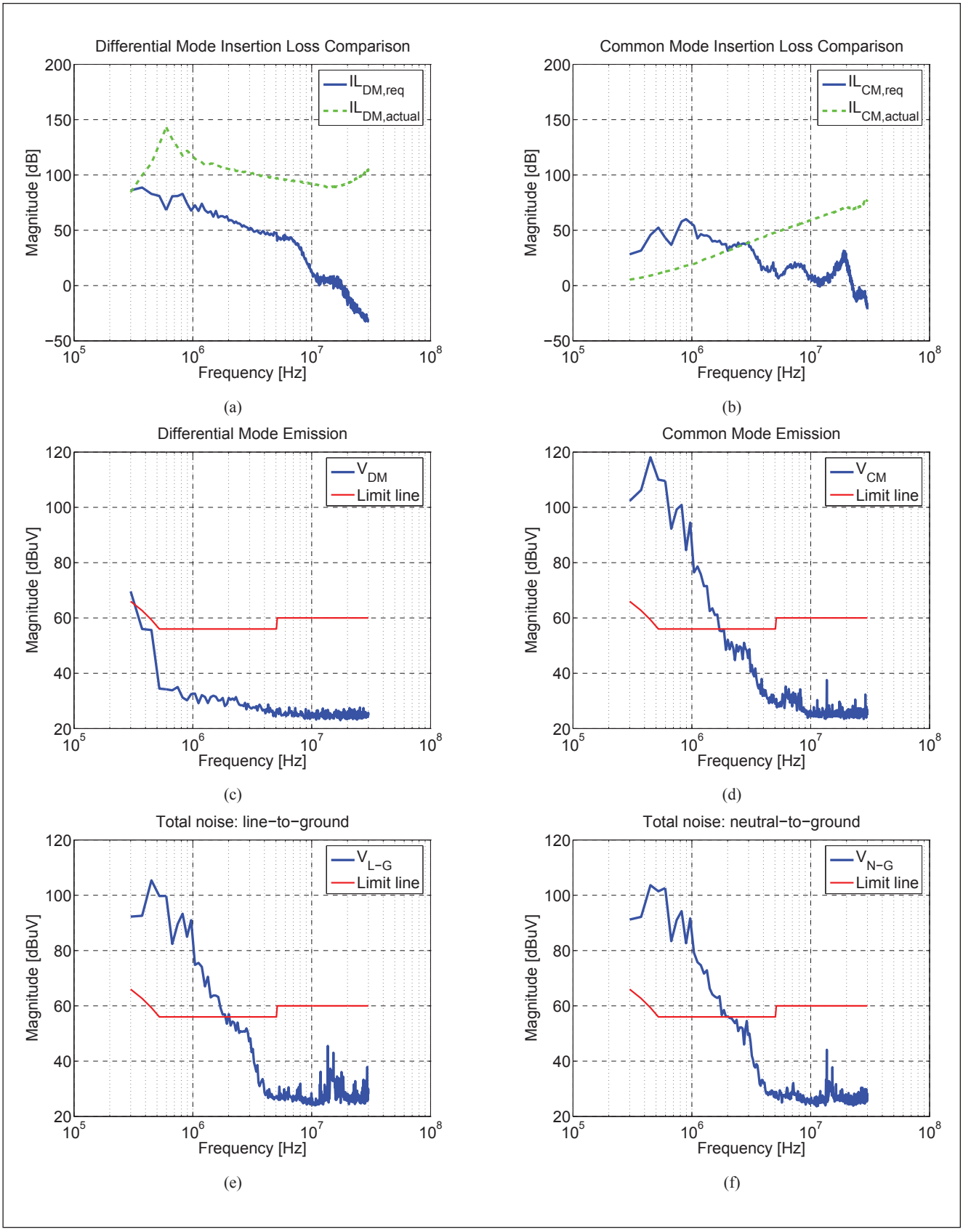

Fig. 13: Non-optimized filter. (a) Required and designed DM insertion losses; (b) required and designed CM insertion losses; (c) measured DM conducted emission; (d) measured CM conducted emission; (e) measured total conducted emission for line-to-ground; (f) measured total conducted emission for neutralto-ground.

References

[1] F.-Y. Shih and et al., "A procedure for designing EMI filters for AC line applications," IEEE Trans. Power Electron., vol. 11, no. 1, pp. 170–181, Jan 1996.
[2] S. Ye, W. Eberle and Y.F. Liu, "A novel EMI filter design method for switching power supplies," IEEE Trans. Power Electron., vol. 19, no. 6, pp. 1668–1678, Nov 2004.
[3] J. J. Goedbloed, Electromagnetic Compatibility, Prentice Hall, 1990.
[4] B. Audone and L. Bolla, "Insertion loss of mismatched EMI suppressors," IEEE Trans. Electromagn. Compat., vol. 20, no. 3, pp. 384–389, Sep 1978.
[5] S. M. Vakil, "A technique for determination of filter insertion loss as a function of arbitrary generator and load impedances," IEEE Trans. Electromagn. Compat., vol. 20, no. 2, pp. 273–278, Sep 1978.
[6] V. Tarateeraseth, Hu Bo, K. Y. See and F. Canavero, "Accurate extraction of noise source impedance of SMPS under operating condition," IEEE Trans. Power Electron., vol. 25, no. 1, pp. 111–117, Jan 2010.
[7] V. Tarateeraseth, K. Y. See, F. Canavero and R.W.Y. Chang, "Systematic electromagnetic interference filter design based on information from in-circuit impedance measurement," IEEE Trans. Electromagn. Compat., vol. 52, no. 3, pp. 588–598, Aug 2010.
[8] V. Tarateeraseth, K. Y. See, L.B. Wang and F.G. Canavero, "Systematic Power Line EMI Filter Design for SMPS," Proc. of 10th International Symposium on EMC (EMC Europe 2011), York (UK), pp. 586-591, September 26 30, 2011.
[9] Clayton R. Paul, Introduction to Electromagnetic Compatibility, John Wiley & Sons, second edition, 2006. [10] Tim Williams, EMC for product designers, Newnes, forth edition, 2007.
[11] M. J. Nave, Power Line Filter Design for Switched Mode Power Supplies, New York: Van Nostrand Reinhold, 1991.
[12] L. Tihanyi, Electromagnetic Compatibility in Power Electronics, IEEE Press, 1997.
[13] S. Wang, F. C. Lee, D. Y. Chen and W. G. Odendaal, "Effects of parasitic parameters on EMI filter performance," IEEE Trans. Power Electron., vol. 19, no. 3, pp. 869–877, May 2004.
[14] S. A. Pignari and A. Orlandi, "Long-cable effects on conducted emissions levels," IEEE Trans. Electromagn. Compat., vol. 45, no. 1, pp. 43–54, Feb 2003.
[15] S. Wang, J. D. Van Wyk and F. C. Lee, "Effects of interactions between filter parasitic and power interconnects on EMI filter performance," IEEE Trans. Power Electron., vol. 54, no. 6, pp. 3344–3352, Dec 2007.
[16] T. Nussbaumer, M. L. Heldwein and J. W. Kolar, "Differential mode input filter design for a three-phase buck-type PWM rectifier based on modeling of the EMC test receiver," IEEE Trans.Ind. Electron., vol. 53, no. 5, pp. 1649–1661, Oct 2006.
[17] J. C. Shifman, "A Graphical Method for the Analysis and Synthesis of Electromagnetic Interference Filters," IEEE Trans. Electromagn. Compat., vol. 7, no. 3, pp. 297–318, Sep 1965.
[18] B. Garry and R. Nelson, "Effect of impedance and frequency variation on insertion loss for a typical power line filter," in 1998 Proc. IEEE EMC Symposium, pp. 691–695.
[19] K. Y. See, "Network for conducted EMI diagnosis," IEE Electronics Letters, vol. 35, no. 17, pp. 1446–1447, Aug 1999.
[20] M. Kumar and V. Agarwal, "Power line filter design for conducted electromagnetic interference using time-domain measurements," IEEE Trans. Electromagn. Compat., vol. 48, no. 1, pp. 178–186, Feb 2006.
[21] Yuang-Shung Lee, Yu-Lin Liang, and Ming-Wang Cheng, "Time Domain Measurement System for Conducted EMI and CM/DM Noise Signal Separation," International Conference on Power Electronics and Drives System, vol. 2, 2005, pp. 1640–1645.
[22] H. J. Chiu, T. F. Pan, C. J. Yao and Y. K. Lo, "Automatic EMI Measurement and Filter Design System for Telecom Power Supplies," IEEE Trans. Instrum. Meas., vol. 56, no. 6, pp. 2254–2261, Dec 2007.
[23] S.Wang, R. Chen, J.D. vanWyk, F. C. Lee, and W.G.Odendaal, "Developing parasitic cancellation technologies to improve EMI filter performance for switching mode power supplies," IEEE Trans. Electromagn. Compat., vol. 47, no. 4, pp. 921–929, Nov 2005.
[24] T. C. Neugebauer and D. J. Perreault, "Parasitic capacitance cancellation in filter inductors," IEEE Trans. Power Electron., vol. 21, no. 1, pp. 282–288, Jan 2006.
[25] T. C. Neugebauer and D. J. Perreault, "Filters and components with inductance cancellation," IEEE Trans. Ind. Appl., vol. 40, no. 2, pp. 483–490, Mar./Apr. 2004.
[26] D. M. Mitchell, DC-DC Switching Regulator Analysis, McGraw-Hil, 1988, ch. 4.
[27] Limits and Methods of Measurement of Radio Interference Characteristics of Information Technology Equipment, CISPR 22, 2004.
[28] R. L. Ozenbaugh, EMI Filter Design, Marcel Dekker, second edition, 2001.
[29] S. Wang, F. C. Lee, and J.D. Van Wyk, "A study of integration of parasitic cancellation techniques for EMI filter design with discrete components," IEEE Trans. Power Electron., vol. 23, no. 6, pp. 3094–3102, Nov 2008.
[30] D. Zhang, D. Y. Chen, M. J. Nave and D. Sable, "Measurement of noise source impedance of off-line converters," IEEE Trans. Power Electron., vol. 15, no. 5, pp. 820–824, Sep 2000.

Biography

Vuttipon Tarateeraseth *received the B. Eng. (second-class honors) and M. Eng. degree both in electrical engineering from King's Mongkut Institute of Technology Ladkrabang (KMITL), Thailand, and Ph.D. in electronics and communications engineering from Politecnico di Torino, Italy. Since 2011, he is a lecturer at Department of Electrical Engineering, Srinakharinwirot University, Thailand. From 2010-2011, he was a lecturer at College of Data Storage Innovation, KMITL. Prior to 2007, he worked as a head of environment testing laboratory at Delta Electronics (Thailand) for three years. He also worked as an EMC engineer for 2 years under the Joint Development of Teaching Materials to Improve EMC Skills of Academic Staff and Postgraduate Electronic Designers Project funded by European Commission. His research interests are mainly in the fields of EMI reduction techniques, EMC/EMI modeling, EMC instruments and measurements and EMI filter design. He is author or coauthor of more than 40 technical papers published in international journals and conference proceedings and one book chapter.*